

## TWO RECENT EXPERIMENTS AT GAMMASPHERE \* \*\*

R.M. DIAMOND

Nuclear Science Division  
Lawrence Berkeley Laboratory  
Berkeley, California 94720, USA

*(Received December 10, 1996)*

Two Gammasphere experiments of the past year are described to illustrate the new capabilities possible. One involves lifetime measurements on M1 bands in  $^{198,199}\text{Pb}$  to see if the predictions of the TAC model of Frauendorf for  $B(\text{M1})$  values of the “shears bands” hold experimentally. The other is a search for discrete linking transitions between the superdeformed and normal deformed bands in  $^{194}\text{Pb}$  in order to determine the spins, parity, and excitation energy of the superdeformed band.

PACS numbers: 27.80. +w, 23.20. Lv, 23.10. Re, 21.10. Tg

**1.  $B(\text{M1})$  values in M1 bands in  $^{198,199}\text{Pb}$** 

Regularly-spaced rotational bands with curious properties were found in light Pb isotopes starting around 1992 [1–3], and now more than 35 such bands have been seen from  $^{194}\text{Pb}$  to  $^{202}\text{Pb}$ . It was striking to observe such nice rotational bands in the semi-magic Pb nuclei. It was even stranger when it was realized that the intraband transitions were stretched M1's and not E2's as in normal rotational bands. Other characteristics were also puzzling; these transitions had reduced transition probabilities,  $B(\text{M1})$ 's, that were large, of order  $1\text{--}4 \mu_N^2$ , among the largest yet observed for medium or heavy nuclei. And the crossover E2 transitions were weak or not observed at all, with small  $B(\text{E2})$  values of  $\sim 0.1 (\text{eb})^2$ , leading to small values of the quadrupole moment and of the deformation,  $\beta_2 \sim 0.1$ . The dynamic moments of inertia,  $J^2$ , of these bands are generally of order  $20 \hbar^2/\text{MeV}$ , giving a ratio of  $J^2/B(\text{E2})$  of  $200 \hbar^2/\text{MeV}$  or more. This is roughly an order

---

\* Presented at the XXXI Zakopane School of Physics, Zakopane, Poland, September 3–11, 1996.

\*\* The work reported was supported in part by the U.S. Department of Energy through Contract No. DE-AC03-76SF (LBL) and Contract No. W-7405-ENG-48 (LLNL).



allel to the nuclear symmetry axis while the  $i_{13/2}$  neutron holes' angular momentum vector,  $j_\nu$ , has aligned with the rotation axis; they are essentially perpendicular to each other. The total angular momentum vector,  $J$ , then lies along a tilted axis at an angle  $\theta$  with respect to the symmetry axis. Since in the present situation  $j_\pi$  and  $j_\nu$  are almost equal in magnitude, and  $R$ , the collective angular momentum of the remaining valence nucleons is small ( $1-7 \hbar$  from low- $j$   $p, f$  neutron orbitals), the angle  $\theta$  is near  $45^\circ$ . An increase in angular momentum and energy in going up the band occurs by a simultaneous closing of the vectors of both pairs of particles towards  $J$ , keeping  $\theta$  about the same but lengthening  $J$ . The name "shears band" comes from the similarity to the closing of the blades of a shears. Only a small component of the total angular momentum is from collective rotation, but if the angular momentum vectors of the described high- $j$  proton and neutron pairs are long enough at the bandhead, then monotonically increasing transition energies roughly proportional to the total spin  $J$  are predicted for a cascade of 6-10 transitions, as is seen experimentally. The calculations also make predictions about the  $B(M1)$  values for these transitions. First, they will be large, because the transverse M1 moments of the high- $j$  protons and high- $j$  neutron holes add to a large value, and second, the  $B(M1)$  values will decrease in a calculable way with an increase in spin as the transverse moment decreases.

So attempts have been made to determine the magnitude of  $B(M1)$ s for particular bands by means of DSAM lifetime measurements [8-12]. However, these early experiments suffered from rather poor statistics and have been inconclusive, some even contradictory. But now with the much increased sensitivity of Gammasphere, Eurogam, and Gasp, we can achieve better statistics and make a better test of the TAC predictions. We have repeated the DSAM experiments to determine the lifetimes of states in two M1 bands in both  $^{198}\text{Pb}$  and in  $^{199}\text{Pb}$  [13]. These bands were produced simultaneously using the  $^{186}\text{W}(^{18}\text{O}, xn)$  reaction at 99 and at 104 MeV. The beam from the 88-Inch Cyclotron of the Lawrence Berkeley Laboratory bombarded a  $0.50 \text{ mg/cm}^2$   $^{186}\text{W}$  foil on a  $0.70 \text{ mg/cm}^2$  Al backing at 99 MeV, and at 104 MeV a  $12.2 \text{ mg/cm}^2$  thick  $^{186}\text{W}$  target. Gamma rays were detected by Gammasphere [14] which at that time consisted of 60 (75-80%) Ge detectors, principally at six angles. There were  $1.9 \times 10^9$  triple- and higher-fold events and  $4.7 \times 10^8$  quadruple- and higher- fold events collected with the Al-backed and thick targets, respectively.

The data were sorted into gated, angle-dependent spectra and  $E_\gamma$ - $E_\gamma$  correlation matrices. All lines in the M1 bands of  $^{198,199}\text{Pb}$  appeared at their fully stopped positions in the thick-target data, and these spectra were used to obtain M1 branching ratios for the in- band transitions. With the Al-backed target, Doppler-broadened lineshapes were observed for in-band

transitions with energies  $\geq 350$  keV. From these lineshapes, level lifetimes were obtained using the analysis program of Wells and Johnson [15].

There is rather good agreement of the calculated shapes with those of the experimental spectra, and the lifetimes obtained for the states in the four bands are given in Table I.

TABLE I

Measured lifetimes,  $\tau(ps)$ , M1 branching ratios,  $B_\gamma$ , and reduced transition strengths,  $B(M1)(\mu_N^2)$  and  $B(E2)(e^2b^2)$ , of states in the bands. The errors on the  $B(M1)$  and  $B(E2)$  values were estimated from the standard (linear) transformation of the errors on the values of  $\tau$  and  $B_\gamma$ . Note, systemic errors introduced through the treatment of the stopping powers are not included.

	$E_\gamma^{M1}$ (keV)	$E_\gamma^{E2}$ (keV)	$\tau$ (ps)	$B_\gamma$	$B(M1)$ ( $\mu_N^2$ )	$B(E2)$ ( $e^2b^2$ )
$^{198}\text{Pb}(1)$	506	970	$0.20^{+0.05}_{-0.05}$	0.90(2)	$1.85^{+0.46}_{-0.46}$	$0.048^{+0.015}_{-0.015}$
	464	885	$0.14^{+0.03}_{-0.04}$	0.90(2)	$3.14^{+0.84}_{-0.63}$	$0.101^{+0.034}_{-0.029}$
	421	795	$0.15^{+0.03}_{-0.04}$	0.94(2)	$3.36^{+0.71}_{-0.54}$	$0.081^{+0.032}_{-0.030}$
	374	699	$0.14^{+0.03}_{-0.04}$	0.89(3)	$5.90^{+1.70}_{-1.28}$	$0.384^{+0.152}_{-0.133}$
$^{198}\text{Pb}(3)$	471	915	$0.20^{+0.06}_{-0.05}$	0.88(2)	$2.33^{+0.62}_{-0.74}$	$0.081^{+0.025}_{-0.028}$
	444	866	$0.20^{+0.08}_{-0.06}$	0.86(2)	$2.31^{+0.63}_{-0.84}$	$0.107^{+0.033}_{-0.042}$
	422	811	$0.17^{+0.06}_{-0.04}$	0.86(2)	$3.06^{+0.64}_{-0.97}$	$0.173^{+0.044}_{-0.060}$
	389	731	$0.24^{+0.05}_{-0.05}$	0.94(2)	$3.17^{+0.64}_{-0.64}$	$0.094^{+0.037}_{-0.037}$
	342	621	$0.16^{+0.08}_{-0.06}$	0.90(3)	$5.82^{+1.95}_{-2.59}$	$0.487^{+0.218}_{-0.261}$
$^{199}\text{Pb}(1)$	508	967	$0.21^{+0.06}_{-0.05}$	0.86(2)	$1.66^{+0.40}_{-0.48}$	$0.065^{+0.018}_{-0.021}$
	459	870	$0.15^{+0.05}_{-0.04}$	0.93(2)	$2.95^{+0.70}_{-0.87}$	$0.068^{+0.025}_{-0.028}$
	411	774	$0.16^{+0.05}_{-0.04}$	0.90(2)	$4.35^{+1.16}_{-1.45}$	$0.197^{+0.066}_{-0.077}$
	363	679	$0.20^{+0.05}_{-0.05}$	0.90(2)	$4.82^{+1.27}_{-1.27}$	$0.300^{+0.099}_{-0.099}$
$^{199}\text{Pb}(2)$	573	1105	$0.14^{+0.03}_{-0.02}$	0.84(2)	$1.51^{+0.19}_{-0.29}$	$0.050^{+0.009}_{-0.011}$
	532	1014	$0.13^{+0.04}_{-0.03}$	0.85(2)	$1.89^{+0.36}_{-0.47}$	$0.072^{+0.017}_{-0.020}$
	482	912	$0.16^{+0.05}_{-0.03}$	0.90(2)	$2.22^{+0.35}_{-0.59}$	$0.069^{+0.018}_{-0.023}$
	430	807	$0.21^{+0.04}_{-0.03}$	0.89(2)	$2.59^{+0.36}_{-0.47}$	$0.120^{+0.027}_{-0.031}$

From the mean lives,  $\tau$ , and the values of the experimental M1 branching,  $B_\gamma = \text{Int}_{M1}/(\text{Int}_{M1} + \text{Int}_{E2})$ , given in the Table, values of the experimental reduced transition probabilities,  $B(M1)$  and  $B(E2)$ , can be calculated by the standard formulae [16],

$$B(M1) = \frac{0.05697 B_\gamma}{E_\gamma^3 \tau (1 + \alpha_{\text{TOT}})} [\mu_N^2],$$

$$B(E2) = \frac{0.08156(1 - B_\gamma)}{E_\gamma^5 \tau (1 + \alpha_{\text{TOT}})} [e^2 b^2],$$

where  $\tau$  is in picoseconds and  $E_\gamma$  is the transition energy in MeV. The  $\Delta I = 1$  transitions were assumed to be pure M1, which assumption is supported by previous studies which generally found very small mixing ratios. These experimental reduced transition probabilities are also given in Table I and the  $B(M1)$  values are shown in Fig. 2 along with the TAC calculations for the assumed configurations. The nomenclature for the bands is that usually employed [5, 12], in which A,B,C,D represent the intruder  $i_{13/2}$  neutron-hole orbitals, E,F represent normal-parity  $p, f$  neutron states, and 8 and 11 stand for (the spins of) the proton pair. It should be mentioned that the spins and configurations of the two bands in  $^{199}\text{Pb}$  are firmly established by earlier

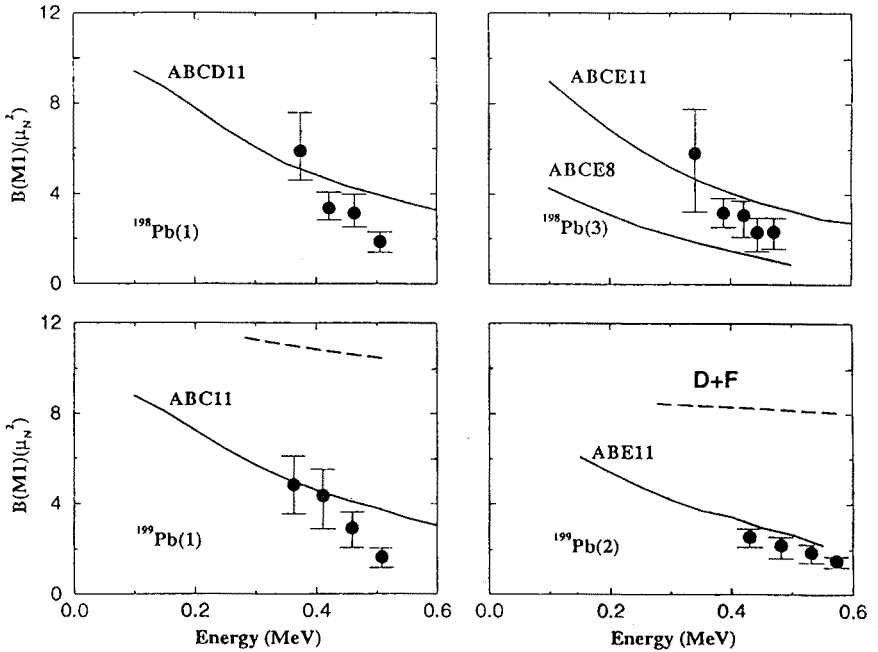


Fig. 2. Experimentally deduced  $B(M1)$  values, plotted as a function of transition energy, for the bands in  $^{198,199}\text{Pb}$  as discussed in the text. The solid lines are the results of TAC model calculations [12] for the suggested configurations of the bands. Note that for  $^{198}\text{Pb}(3)$  two possible configurations have been considered. For the  $^{199}\text{Pb}$  bands (Fig. 2c,d), the dashed lines are  $B(M1)$  estimates calculated using the semi-classical treatment of Dönau and Frauendorf [17].

work, but those of  $^{198}\text{Pb}$  are tentative. Also shown for the  $^{199}\text{Pb}$  bands are  $B(\text{M}1)$  values calculated using the earlier semi-classical expression of Donnau and Frauendorf [17]. Clearly the TAC calculations are the better fits, and even reasonably good.

In the past, long, regular rotational bands have been taken as an indication of a substantial quadrupole deformation in the nucleus. So that now the idea seems natural to us that a substantial deformation is necessary for a long and regular rotational band. But that may not be so. A (large) quadrupole deformation permits specification of an orientation of the nuclear quadrupole moment with respect to an axis of rotation, as illustrated in Fig. 3; the rotational symmetry of the nucleus has been broken. And this means that the orientation can change, the nucleus can rotate. (If the combined effects of the rotation on the nuclear deformation, on the pairing correlations, on the nucleonic alignment, etc. make only small changes in the moment of inertia, the resulting motion resembles that of a rigid rotor. Superdeformed bands are excellent examples. But of course the nucleus is not rigid.) The rotating deformed charge distribution emits electric quadrupole radiation which connect the states of the band and decrease the energy and angular momentum of the nucleus. But there is another possible way to specify the nuclear orientation, even if the nucleus is only slightly (oblate) deformed as in the situation we have been discussing. If the angular momentum vector of a few high- $j$  protons and that of a few high- $j$  neutron holes, or vice-versa, are near right angles to each other, there is a large magnetic dipole-moment component perpendicular to the total angular momentum. This again specifies an orientation with respect to the latter, so again rotational symmetry is broken. But now it is a magnetic dipole component that rotates and emits magnetic dipole radiation to cool the nucleus down the band. And so the name magnetic rotation [7] has been suggested to contrast this situation with the more usual electric rotation with the emission of quadrupole radiation. The requirements are quite different. The quadrupole deformation is the collective result of the valence nucleons. But to create a large transition magnetic dipole moment only a couple of high- $j$  protons and one, two, or three high- $j$  neutron holes, or vice-versa, are needed. And for this latter case, only a slight quadrupole polarization or deformation of the core along with the direct p-n interaction (degree of overlap) of these high- $j$  particles and holes gives the resistance to change characterizing the moment of inertia and yielding a gradual and regular closing of the "shears". Finally, an interesting point that remains is, what happens when the high- $j$  protons and neutron holes are maximally aligned (parallel)? Is there a band termination? In the present experiment the two bands in  $^{199}\text{Pb}$  were observed to higher spins than before: two levels more to probable spin  $63/2$  for band 1, and seven more to probable spin  $75/2$


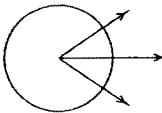
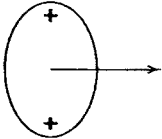
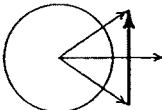
Electric and Magnetic Rotation		
$\Delta I = 2$ ordinary bands	Characteristic of rotational bands	$\Delta I = 1$ shears bands
 <p>gradual alignment of many short vectors</p>	<p>regular <math>E_\gamma \propto I</math></p>  <p>gradual alignment of few long vectors</p>	
<b>E2</b>	enhanced transitions	<b>M1</b>
 <p><b>electric quadrupole</b> mass distribution</p> <p>classic and quantal</p>	<p>possibility to define the orientation (with respect to the a. m. vector)</p> <p>large isotropy broken "inertia" <math>J^{(2)} = \Delta\omega/\Delta E_\gamma</math></p>	 <p><b>magnetic dipole</b> current distribution</p> <p>quantal</p>
<b>electric</b>	<b>rotation</b>	<b>magnetic</b>

Fig. 3. The relation between electric and magnetic rotation

for band 2. Band 1 shows a band crossing, thought to be  $A11 \rightarrow ABC11$  (in agreement with the experimental alignment of  $\sim 8 \hbar$ ), but above that is regular. The maximum spin possible for  $ABC11$  is  $(33/2 + 11) = 55/2$  plus a small collective rotation contribution. Taking that as 4 from TAC calculations, the terminal spin for this configuration is  $63/2$ . That is the highest spin actually observed, with a sharp drop in intensity for any discrete lines above it. A similar estimate for band 2,  $ABE11$ , gives  $(29/2 + 11) = 51/2$ , plus  $\sim 3$  (collective) makes  $57/2$  for termination. This is just where a splitting of the band and a crossing occur, probably to  $ABCDE11$ . If so, this band would terminate at approximately the highest spin observed for it,  $73/2$ , or one or two states higher.

In summary, it seems that “regular” rotational bands can appear without the necessity of strong electric quadrupole collectivity (deformation). In the light Pb nuclei as few as two high- $j$  protons and two high- $j$  neutron holes can give rise to “magnetic rotation”, a new mode of nuclear excitation. In this process a large magnetic-dipole moment breaks the rotational symmetry of the nucleus and causes strong M1 transitions between the members of a  $\Delta I = 1$  band whose transition energies increase monotonically with spin, but are not collective in the usual sense. The lifetimes determined in the present experiment are accurate enough to indicate that the TAC calculations give a good account of this type of behavior. Thus the study of these interesting bands have widened our understanding and thinking about “rotational” and “collective” excitations.

## 2. Discrete linking transitions in $^{194}\text{Pb}$

Despite the wealth of information that exists now on superdeformed (SD) bands, some of their most important properties have not yet been determined experimentally, *e.g.*, spins, parity, and excitation energy. The observation of discrete transitions linking the SD and known, low-lying normal deformed (ND) states, if successful, would yield these crucial data, and thus provide benchmarks for the theorists doing calculations on SD band properties and regions. In addition, this information is necessary for a more detailed understanding of the de-excitation process itself.

The difficulty in finding SD linking transitions is that there are too many of them; there are a very large number of pathways down from the ND level or levels at several MeV excitation energy which are mixed slightly with each decaying SD state, a whole continuum of few-step to many-step paths. There are, however, a small number of transitions that go in one large jump (of 2–5 MeV in the mass-190 region) down to a small number of low-lying levels near the ground state of similar spin to the decaying SD level (within one or two units). These are what I shall call primary or, not very accurately, “one-step” transitions, and they have the best chance of any discrete path to be observed. This is because they appear in a higher energy region of the  $\gamma$ -ray spectrum, of relatively low and smooth background with few other discrete peaks nearby. The resolving power and efficiency of the new generation of Ge arrays allows the possible realization of observing these transitions. Brinkman *et al.* [18] used the Early Implementation mode of Gammasphere with 32 detectors to study  $^{194}\text{Pb}$ , and found a single candidate  $\gamma$ -ray of 2.746 MeV linking the yrast SD band to the  $6^+$  state 2.136 MeV above the  $0^+$  ground state. When the array had grown to 55 detectors, Khoo *et al.* [19] studied  $^{194}\text{Hg}$  and found four links between the yrast SD band there and the low-lying ND levels, and so determined the excitation



energies and spins of the SD band. Then the present collaboration, utilizing Gammasphere now with 88 detectors, repeated the search in  $^{194}\text{Pb}$ , and this is the study I want to tell you about [20]. The hope was to not only confirm the link of the earlier work, but to find still more. Another study of  $^{194}\text{Pb}$  was performed in parallel to ours at Eurogam, and has been published recently [21] with similar, but somewhat less extensive, results.

The experiment was performed at the 88-Inch Cyclotron of the Lawrence Berkeley Laboratory, using the  $^{174}\text{Yb}(^{25}\text{Mg}, 5n)^{194}\text{Pb}$  reaction at 130 MeV. The isotopically enriched ( $> 98\%$   $^{174}\text{Yb}$ ) target was  $1.21\text{ mg/cm}^2$  thick, and had been evaporated onto a  $6.13\text{ mg/cm}^2$  Au backing. Since the lower-lying SD states have lifetimes that are longer than the stopping times of the evaporation products in the backing, the linking transitions should not show Doppler broadening and the intrinsic detector resolution was expected, and found. Approximately  $7 \times 10^9$  events were recorded for Compton-suppressed Ge folds  $\geq 4$ .

The search for linking transitions was performed using a RadWare cube [22] whose generation required that each event in the cube had been gated by one or more transition energies of the  $^{194}\text{Pb}$  SD band, excluding the 419.9 keV  $\gamma$ -ray because of its nearness to the 421.1 keV,  $7^- \rightarrow 5^-$  low-lying transition. The cube transitions were also required to be in prompt coincidence with respect to the beam pulse. Energy and efficiency calibrations over the range 0.100–3.548 MeV were obtained from standard  $^{56}\text{Co}$ ,  $^{152}\text{Eu}$ , and  $^{182}\text{Ta}$  sources. Figure 4 illustrates two energy regions of an additionally doubly SD-band-gated, background-subtracted projection from the cube; all possible combinations of double gates on the SD lines between 170 and 532 keV, inclusive, were summed to produce this spectrum. The top part of the figure shows that a number of  $\gamma$ -ray transitions from low-lying ND states in  $^{194}\text{Pb}$ , labeled by their spin change, are in coincidence with the SD cascade, and are the final steps in the decay-out. More interesting for us is the high-energy (b) part of the spectrum, where there appear of order two dozen candidates for discrete primary transitions feeding into the low-lying ND states just described.

Coincidence relationships between the yrast SD transitions and either the candidate primaries or the low-lying  $\gamma$ -rays were studied to verify which, indeed, are linking transitions, and to place them in the  $^{194}\text{Pb}$  level scheme [23]. For example, Fig. 5(a) shows the sum of all double-gate combinations on the RadWare cube between the 2743 keV transition and all the yrast SD band transitions. It can be seen that the 2743 keV  $\gamma$ -ray depopulates the band below the 170 keV SD transition since the 170 keV line is observed. Another important feature is the strong enhancement of the 595 keV  $6^+ \rightarrow 4^+$  low-lying transition in comparison with the triply SD-gated spectrum in Fig. 4(a). This indicates that the 2743-keV transition decays into, or

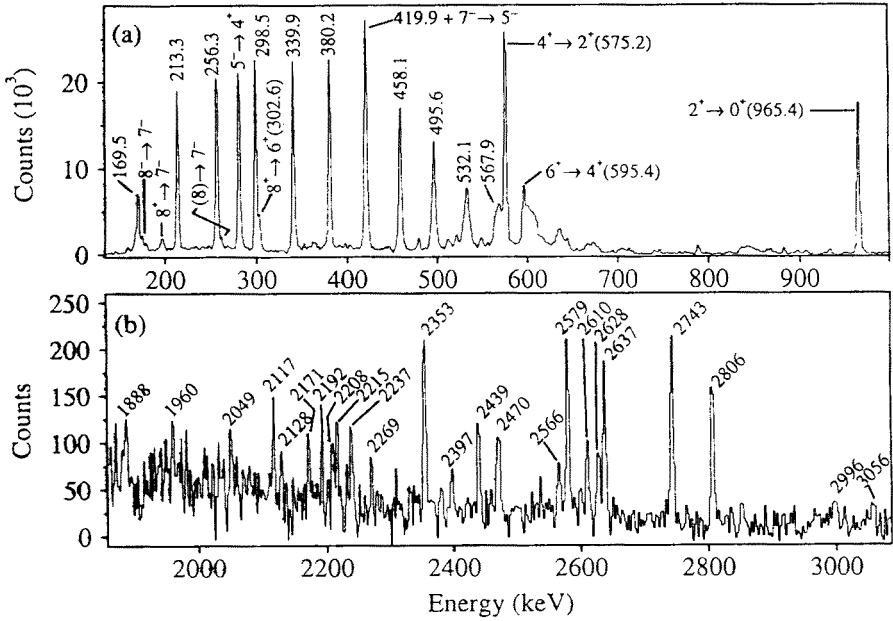


Fig. 4. Background-subtracted, coincidence spectra obtained from the singly-gated cube by summing the spectra from all pairwise gate combinations possible with the 170 to 532 keV yrast SD transitions. Exclusion of the 419 keV SD line from the gate list used to create the cube helps result in its apparent increased intensity. The low-energy portion of the spectrum; (a) — displays the yrast SD band members (energies in keV) and coincident low-lying ND transitions (labeled by  $(J^\pi)_i \rightarrow (J^\pi)_f$  at the end of the de-excitation paths, while (b) — presents the candidate primary transitions directly linking the SD states and the lowest ND levels.

above, the 6<sup>+</sup> state. Figures 5(b) and 5(c) present low- and high-energy regions, respectively, of spectra obtained by the sum of double gates on the 595 keV and the in-band SD transitions. It is apparent from these spectra that the 595 keV  $\gamma$ -ray is in coincidence with the SD band, the 303 keV 8<sup>+</sup> → 6<sup>+</sup> transition, and the 2117-, 2353-, 2470-, 2610-, and 2743-keV primary transitions. A full-resolution RadWare cube was also sorted in order to build a more complete low-lying level scheme from the present high-statistics data. The resulting scheme is essentially that of Refs [24, 25] with the addition of six transitions observed in Ref. [26], four of which were placed in the current work, and additional states at 2408 and 3374 keV. All twelve candidate primaries were placed with the aid of the revised decay scheme for <sup>194</sup>Pb, although four of the levels are of unknown spin and parity. The results are shown in Fig. 6.

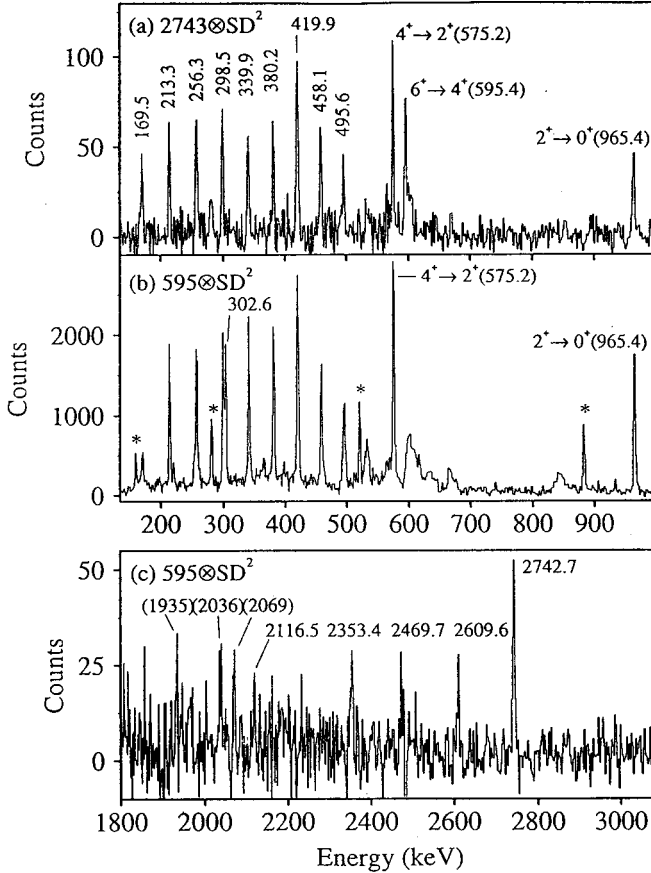


Fig. 5. Coincidence spectra projected from a SD-gated cube obtained from the summation of pairwise gates between the SD band members and: (a) the 2743 keV primary transition, (b), (c) the 595 keV yrast  $6^+ \rightarrow 4^+$  transition. An asterisk denotes a contaminant from  $^{193}\text{Pb}$  brought in by the  $213 \times 595$  keV gate.

Possible multiplicities of these lines, and of the SD transitions themselves, were deduced from empirical asymmetry ratios,

$$R_{\text{asym}} = \text{Intensity}(\text{forward and backward}) / \text{Intensity}(\overline{90^\circ}).$$

Matrices were constructed which contained  $\gamma$ - $\gamma$  coincidences between any detector with: 1) detectors at the three most forward angles ( $17.3^\circ$ ,  $31.7^\circ$ ,  $37.4^\circ$ ) and three most backward angles ( $142.6^\circ$ ,  $148.3^\circ$ ,  $162.7^\circ$ ) with respect to the beam line, and 2) detectors around  $\overline{90^\circ}$  ( $69.8^\circ$ ,  $79.2^\circ$ ,  $80.7^\circ$ ,  $90.0^\circ$ ,  $99.3^\circ$ ,  $100.3^\circ$ ,  $110.2^\circ$ ). The asymmetry ratio, normalized by the ratio of the number of detectors at  $\overline{90^\circ}$  to the number at (forward + backward)

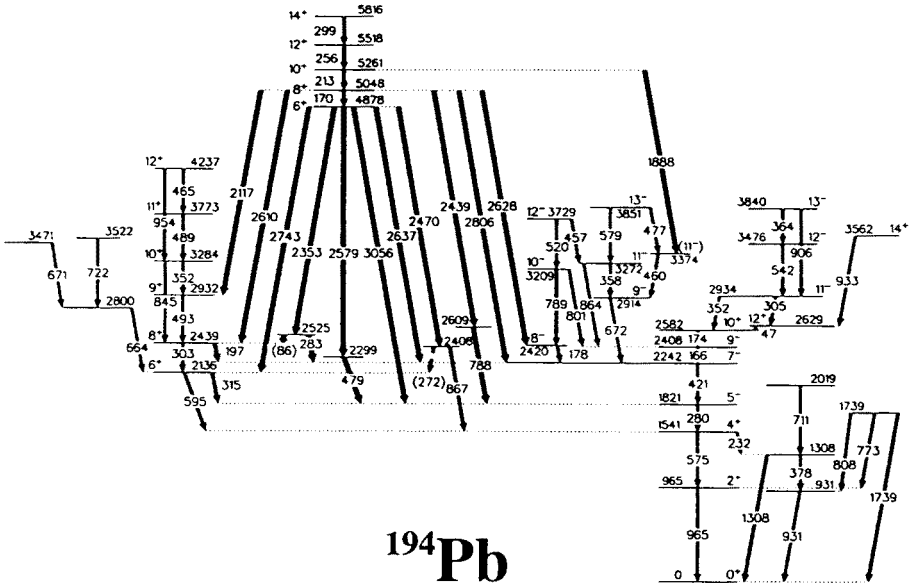


Fig. 6. Discrete decay paths out of the  $^{194}\text{Pb}$  yrast SD band. Levels are labeled by  $E_x$  in keV and  $J^\pi$ . Transition energies are given in keV. For clarity, only ND states in the immediate region of the end-points of the primary transitions are shown.

angles used, was deduced for relevant  $\gamma$ -rays in these matrices, and those of the primary transitions are given in Table II. The mean  $R_{\text{asym}}$  values of known low-lying stretched  $L = 2$  and  $L = 1$  transitions are 1.35(3) and 0.71(2), respectively, and the mean value obtained for the intraband SD transitions is 1.43(2), confirming their stretched E2 character. One should note that just using these ratios it is not possible to distinguish 1) between  $\Delta L = 1$ ,  $\Delta J = 1$  and  $\Delta L = 2$ ,  $\Delta J = 0$  transitions, or 2) between  $\Delta L = 1$ ,  $\Delta J = 0$  and  $\Delta L = 2$ ,  $\Delta J = 2$  transitions. Nevertheless, these ratios can be used to place restrictions on the multiplicities of the primary transitions and, since the final spin and parity is known in most cases, limits on the spin and parity of the initial state in the SD band can be set. Examination of these initial  $J^\pi$  values for the SD levels involved in the linking transitions, Table II, indicates that the two lowest observed SD states can only be assigned  $J^\pi = 6^+$  and  $8^+$ , respectively. This is without making any assumptions about the SD band. It is worth noting that these spins are in agreement with those calculated (predicted) years ago in Ref. [27].

TABLE II

The primary decay data:  $E_\gamma^a$ ,  $I_\gamma$ ,  $R_{\text{asym}}$ ,  $J_\pi^\pi$ ,  $\sigma L$  and reduced transition probabilities  $B(\sigma L)$ .

$E_\gamma$ (keV)	$I_\gamma$ (%)	$R_{\text{asym}}$	$\sigma L$	$J_\pi^\pi$	$J_\pi^\pi$	favoured $\sigma L$	$B(\sigma L)$ (W.U)
Decays out of the third lowest SD level ( $J_\pi^\pi = 10^+$ )							
1887.9(3)	1.0(4)	0.9(1)	$\Delta L = 1, \Delta J = 1$ or $\Delta L = 2, \Delta J = 0$	$11^-$	$10^+, 11^-, 12^+$	(E1)	$5(2) \cdot 10^{-8}$
Decays out of the second lowest SD level: $J_\pi^\pi = 8^+$							
2116.5(4)	0.9(5)	0.3(1)	mixed M1/E2	$9^+$	$8^+, 9^+, 10^+$	M1/E2	-
2438.5(4)	0.9(4)	1.0(2)	mixed M1/E2	-	-	-	-
2609.6(4)	1.7(6)	1.4(3)	$\Delta L = 1, \Delta J = 0$ or $\Delta L = 2, \Delta J = 2$	$8^+$	$6^+, 8^+, 10^+$	M1	$2.3(9) \cdot 10^{-6}$
2627.9(4)	1.3(6)	1.4(3)	$\Delta L = 1, \Delta J = 0$ or $\Delta L = 2, \Delta J = 2$	$8^-$	$6^-, 8^+, 10^-$	E1	$1.6(7) \cdot 10^{-8}$
2806.1(3)	1.7(5)	0.7(1)	$\Delta L = 1, \Delta J = 1$ or $\Delta L = 2, \Delta J = 0$	$7^-$	$6^+, 7^-, 8^+$	E1	$1.7(6) \cdot 10^{-8}$
Decays out of the lowest SD level: $J_\pi^\pi = 6^+$							
2353.4(3)	2.8(6)	0.8(1)	$\Delta L = 1, \Delta J = 1$ or $\Delta L = 2, \Delta J = 0$	-	-	-	-
2469.7(4)	1.5(6)	1.4(3)	$\Delta L = 1, \Delta J = 0$ or $\Delta L = 2, \Delta J = 2$	-	-	-	-
2579.1(2)	3.0(6)	0.7(1)	$\Delta L = 1, \Delta J = 1$ or $\Delta L = 2, \Delta J = 0$	-	-	-	-
2636.6(2)	1.8(6)	0.8(2)	$\Delta L = 1, \Delta J = 1$ or $\Delta L = 2, \Delta J = 0$	$7^-$	$6^+, 7^-, 8^+$	E1	$\geq 12(4) \cdot 10^{-8}$
2742.5(2)	3.3(6)	1.1(2)	mixed M1/E2	$6^+$	$5^+, 6^+, 7^+$	M1	$\geq 2.2(5) \cdot 10^{-5}$
3056(1)	0.8(5)	-	-	$5^-$	-	E1	$\geq 4(2) \cdot 10^{-8}$

TOTAL  $I_\gamma = 21(2)\%$  of SD band intensity accounted for by primaries

<sup>a</sup>  $I_\gamma$  is given as a percentage of the SD band population and is corrected for detector efficiency and normalized to the intensity of the 256.3 keV SD line.

The linking-transition data have also allowed the excitation energy of the  $6^+$  SD state to be unambiguously determined for the first time; we find  $E_{\text{exc}}(6^+) = 4.8784(3)$  MeV. Assuming a smooth extrapolation to  $I = 0$ , the  $0^+$  bandhead is estimated to be at 4.641 MeV. This is in surprisingly good agreement with the Hartree-Fock-Bogoliubov calculations of Ref. [28] which predict 4.86 MeV.

Reduced transition probabilities for some of the primary decays have also been calculated from the branching ratio of the primary to the in-band transition competing with it, assuming a constant in-band quadrupole moment,  $Q_t = 20.6(13)$  eb, derived from both DSAM [29] and recoil distance measurements [30]. For the primaries depopulating the  $6^+$  SD state two additional assumptions concerning the unobserved  $6^+ \rightarrow 4^+$  SD transition were necessary: 1) the energy of the transition (124.6 keV) was taken from a smooth extrapolation of the known transition energies; 2) its intensity was estimated to be  $\leq 4\%$  of the plateau region intensity of the SD band. The resulting reduced transition probabilities are highly retarded; typical values are  $B(E1) = \text{few} \times 10^{-8}$  W.u. and  $B(M1) = \text{few} \times 10^{-5}$  W.u. Reasonably similar values were obtained for the four primary E1 transitions found in  $^{194}\text{Hg}$  [19]. However, there are a number of differences between the nature of the linking transitions observed in these two cases. More primaries are found in  $^{194}\text{Pb}$ , 12 compared to 4 in  $^{194}\text{Hg}$ . In the latter case only E1 transitions were seen, while E1, M1, and mixed M1/E2 multipolarities are found in  $^{194}\text{Pb}$  (although more than half of the intensity is E1). A surprisingly large fraction of the  $^{194}\text{Pb}$  SD band decay, 21(2)%, is carried by the primary transitions in contrast to 5% in the Hg case. The main reason for these differences is probably the greater phase space available in the  $^{194}\text{Hg}$  nucleus. The factors that contribute to this are: 1) the excitation energies of the SD bandheads are around 4.64 MeV in  $^{194}\text{Pb}$  and higher, 6.02 MeV, in  $^{194}\text{Hg}$ ; 2) the spins of the SD states at the point of de-excitation and at the end of the primary transition are higher in Hg (10–12) and lower in Pb (6–8); 3) the excitation energy of the ND states into which the primaries decay is of order 2.4 MeV and 2.8 MeV for  $^{194}\text{Pb}$  and  $^{194}\text{Hg}$ , respectively; 4) ND  $^{194}\text{Pb}$  is singly magic, while coexisting prolate and near-spherical bands at low excitation energy further increase the density of ND states in  $^{194}\text{Hg}$  and so can lead to a more fragmented decay. Possibly there are more primary transitions to be found in  $^{194}\text{Hg}$ , but are too weak to have been seen yet. One should also note that the decays of the shape isomers in  $^{236}\text{U}$  are mostly E1 [31] and in  $^{238}\text{U}$  are mostly E2 [32], quite different, even though the ND ground-state bands are almost identical and the excitation energies of the isomers are very similar. Evidently each situation is different, and generalizations about the nature of the primary transitions based on two cases must be viewed cautiously.

In summary, twelve discrete primary  $\gamma$ -ray transitions have been observed linking the three lowest members of the  $^{194}\text{Pb}$  yrast SD band to low-lying ND levels. Anisotropy measurements have shown that these primary transitions include E1, M1, and mixed M1/E2 multipolarities. The two lowest observed SD states have been unambiguously assigned  $J^\pi = 6^+$  and  $8^+$  at excitation energies of 4.878 MeV and 5.048 MeV, respectively, without making assumptions about the properties of SD bands. More such determinations of the  $J^\pi$  and  $E_{\text{exc}}$  values of SD bands, as well as lifetime measurements (where possible) to get quadrupole moments and thus  $B(\text{E}2)$  values, are needed to place more stringent requirements upon theoretical calculations of SD states and their properties, and in particular to address the phenomena of identical bands and of the detailed nature of the tunneling between the two potential wells. The increased sensitivity becoming available with the completion of Gammasphere and Euroball will give us a much better opportunity to obtain these data, and so a much better understanding of these properties can be anticipated.

I am most grateful to Drs. Rod Clark and Karl Hauschild for permitting me to discuss their work before publication, and for many interesting and helpful discussions.

## REFERENCES

- [1] R.M. Clark *et al.*, *Phys. Lett.* **B275**, 247 (1992).
- [2] G. Baldsiefen *et al.*, *Phys. Lett.* **B275**, 252 (1992).
- [3] A. Kuhnert *et al.*, *Phys. Rev.* **C46**, 133 (1992).
- [4] R.M. Clark *et al.*, *Nucl. Phys.* **A562**, 121 (1993).
- [5] G. Baldsiefen *et al.*, *Nucl. Phys.* **A574**, 521 (1994).
- [6] S. Frauendorf, *Nucl. Phys.* **A557**, 259c (1993).
- [7] S. Frauendorf, J. Meng, J. Reif, Proceedings of the Conference on Physics from Large  $\gamma$ -Ray Detector Arrays, Vol. II, Berkeley, California, 1994 (LBL-35687, unpublished) p.52.
- [8] T.F. Wang *et al.*, *Phys. Rev. Lett.* **69**, 21 (1992).
- [9] J.R. Hughes *et al.*, *Phys. Rev.* **C48**, R2123 (1993).
- [10] R.M. Clark *et al.*, *Phys. Rev.* **C50**, 84 (1994).
- [11] E.F. Moore *et al.*, *Phys. Rev.* **C51**, 115 (1995).
- [12] M. Neffgen *et al.*, *Nucl. Phys.* **A595**, 499 (1995).
- [13] R.M. Clark *et al.*, accepted for publication in *Phys. Rev.*
- [14] IY. Lee, *Nucl. Phys.* **A520**, 641c (1990).
- [15] Lineshape: A Computer Program for Doppler-Broadened Lineshape Lifetime Analysis, by J.C. Wells and N. Johnson, private communication. Modified from the original code by J. C. Bacelar.

- [16] H. Ejiri and M.J.A. deVoigt, *Gamma-Ray and Electron Spectroscopy in Nuclear Physics*, Oxford University Press, Oxford, England 1987, p.504.
- [17] F. Döna, S. Frauendorf, Proceedings of the International Conference on High Angular Momentum Properties of Nuclei, Oak Ridge, July, 1982, *Nucl. Sci. Res. Conf. Series*, Vol. 4, Harwood, New York 1983, p. 143.
- [18] M.J. Brinkman, Proceedings of the Conference on Physics from Large  $\gamma$ -Ray Detector Arrays, Berkeley, California, 1994 (LBL 35687, unpublished) p. 242; *Phys. Rev. C* **53**, R1461 (1996).
- [19] T.L. Khoo *et al.*, *Phys. Rev. Lett.* **76**, 1583 (1993).
- [20] K. Hauschild *et al.*, to be published.
- [21] A. Lopez-Martens *et al.*, *Phys. Lett.* **B380**, 18 (1996).
- [22] D.C. Radford, *Nucl. Instrum. Methods Phys. Res. Sect. A* **361**, 306 (1995).
- [23] E. Browne, B. Singh, *Nucl. Data Sheets* **79**, 277 (1996).
- [24] D. Mehta *et al.*, *Z. Phys.* **A345**, 169 (1993).
- [25] M.G. Pourquet *et al.*, *J. Phys. G* **20**, 765 (1994).
- [26] P. van Duppen, E. Coenen, K. Deneffe, M. Huyse, J.L. Wood, *Phys. Rev. C* **35**, 1861 (1987).
- [27] J.A. Becker *et al.*, *Nucl. Phys.* **A520**, 187 (1990); J.E. Draper *et al.*, *Phys. Rev. C* **42**, R1791 (1990).
- [28] S.J. Krieger, P. Bonche, M.L.S. Weiss, J. Meyer, H. Flocard, P.H. Heenen, *Nucl. Phys.* **A542**, 43 (1992).
- [29] P. Willsau *et al.*, *Z. Phys.* **A344**, 351 (1993).
- [30] R. Krücken *et al.*, *Phys. Rev. Lett.* **73**, 3359 (1994).
- [31] J.Schirmer, J. Gerl, D. Habs, D.S. Schwalm, *Phys. Rev. Lett.* **63**, 2196 (1989).
- [32] J. Kantele, W. Stöfl, L.E. Ussery, D.J. Deeman, E.A. Henry, R.J. Estep, R.W. Hoff, L.G. Mann, *Phys. Rev. C* **29**, 1693 (1984).